

KRZYSZTOF PIELICHOWSKI, AGNIESZKA LESZCZYNSKA

Cracow University of Technology
Department of Chemistry and Technology of Polymers
ul. Warszawska 24, 31-155 Kraków, Poland
e-mail: kpielich@usk.pk.edu.pl

Polyoxymethylene-based nanocomposites with montmorillonite: an introductory study

Summary — Nanocomposites of polyoxymethylene (POM) and organo-modified montmorillonite were obtained by melt mixing method and investigated by X-ray diffraction (XRD), scanning electron microscopy (SEM), differential scanning calorimetry (DSC), thermogravimetric analysis (TGA) and mechanical testing, respectively. The XRD results indicated mixed tactoid-exfoliated structure of the obtained nanocomposites; introduction of montmorillonite (MMT) was found to strongly influence the crystalline structure of POM through altering of nucleation mechanism. Layered silicate-modified POM exhibited improved tensile strength and modulus as well as increased elongation, unlike common polymeric microcomposites that reach higher modulus at the expense of ductility. Nanoadditives contribute to the formation of a core-shell morphology of injection-moulded samples that was ascribed to increased elongation at break of nanocomposite materials. Both mechanical and thermal properties of nanocomposites varied depending on type of ammonium surfactant used for organo-modification of MMT.

Key words: polyoxymethylene, organophilization, montmorillonite, nanocomposites, structure, properties.

NANOKOMPOZYTY POLIOKSYMETYLENU Z MONTMORYLONITEM — BADANIA WSTĘPNE
Streszczenie — Nanokompozyty polioksymetyleny (POM) i montmorylonitu (MMT) organofilizowanego za pomocą związków powierzchniowo czynnych typu amin czwartorzędowych (tabela 1) otrzymano metodą homogenizacji w stopionej fazie polimeru (rys. 1). Scharakteryzowano je metodami szerokokątowej dyfrakcji rentgenowskiej (WAXD, rys. 2), skaningowej mikroskopii elektronowej (SEM, rys. 3 i 4), różnicowej kalorymetrii skaningowej (DSC, tabela 2) i analizy termogravimetrycznej (TGA, rys. 8 i 9 i tabela 3) oraz na podstawie testów wytrzymałościowych (rys. 5—7). Wyniki badań strukturalnych świadczą o występowaniu złożonej struktury tych materiałów zawierających zarówno eksfoliowane warstwy MMT, jak i nieinterkalowane pakiety warstw organofilizowanego glinokrzemianu. Dodatek tego ostatniego wywołuje istotne zmiany w budowie krystalicznej POM, zmieniając mechanizm zarodkowania. Nanokompozyty POM z organofilizowanym MMT wykazują zwiększoną wytrzymałość mechaniczną, przy czym w przypadku kompozycji charakteryzującej się największym stopniem homogenizacji obserwowano jednoczesny wzrost wartości wydłużenia przy zerwaniu, w odróżnieniu od mikrokompozytu z niemodyfikowanym MMT, gdzie zwiększonej wytrzymałości mechanicznej towarzyszy zmniejszenie wydłużenia przy zerwaniu. Typ związku amoniowego zastosowanego do modyfikacji MMT wywiera wyraźny wpływ na właściwości mechaniczne i stabilność termiczną kompozytów.

Słowa kluczowe: polioksymetylen, montmorylonit, organofilizacja, nanokompozyty, struktura, właściwości.

Polyoxymethylene (POM) is a semi-crystalline thermoplastic resin with high commercial importance as an engineering polymer [1]. POM is broadly used for manufacturing of construction details where high mechanical, thermal, chemical and electrical performance is required. However, novel POM-based materials are developed to find new application areas and withstand the competition with novel high performance engineering

resins, e.g. polyetheramides [2, 3]. One of the most promising and extensively investigated research areas in that respect is associated with preparation and characterization of POM nanocomposites made of polymeric matrix in which nanoparticles (shapes of which are at least in one dimension under 100 nm) are dispersed. Among different nanoadditives there is a prevailing share of layered silicates, especially montmorillonite

(MMT) which is a natural mineral (clay) in bentonite deposits [4, 5].

Contrary to conventional microcomposites that require few tens wt. % of filler to reach desirable improvement in mechanical properties, nanocomposites offer significant improvement at filler content of only few wt. % [6–8]. Such low-filled polymeric compositions have processing properties similar to this of pristine resin and typical problems of microcomposites' processing, such as changes in melt viscosity or surface roughness of moulded parts, do not occur. Owing to nanometric dimensions of montmorillonite particles (close to the molecular dimensions) large interphase area is achieved at low filler content. Furthermore, when montmorillonite is properly modified and dispersed in the polymer matrix, effective interactions arise between organic and inorganic phase of hybrid material that can cause synergistic effects. Apart from mechanical strength [9] also thermomechanical properties [10], thermal stability [11], flame retardancy [12, 13] and barrier properties [14] were improved successfully by addition of montmorillonite into polymer matrix.

Several methods were elaborated to disperse montmorillonite in polymers — a group from Toyota first proposed a method involving intercalation of monomer into MMT galleries and then exfoliating the layers by subsequent *in situ* polymerization [15]. In another approach MMT water slurry was introduced into polymer melt and the mixture was intensively mixed at high temperature leading to break of MMT packages into individual layers [16]. Other methods utilized the ability of MMT to exchange inorganic cations situated in silicate galleries into organic cations with long hydrocarbon chains that make MMT organophilic [6]. In a case of apolar aliphatic matrices, like polyethylene or polypropylene, additional compatibilizer compound with polar groups was required to disperse organically modified MMT [17].

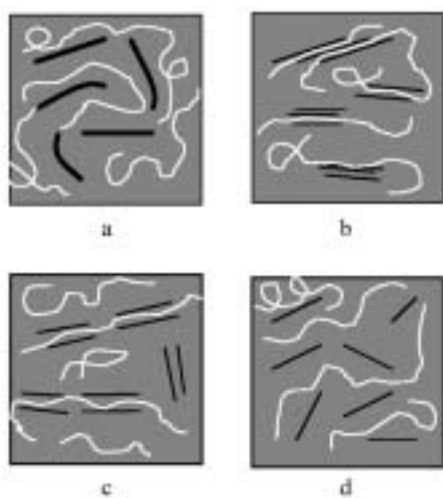


Fig. 1. Schemes of possible polymer-layered silicate nanocomposite structures: a — tactoid; b — intercalated; c — intercalated-flocculated; d — exfoliated (adopted from [18])

Owing to the plate shape of MMT particles, different isotropic and anisotropic structures of nanocomposites may be obtained depending on composition and method/conditions of preparation (Fig. 1).

Through the last decade nanocomposites with most of the large-scale produced polymers (*e.g.* PE, PP, PA, PS, PVC or PC) were obtained and characterised, but there are only few works presented in literature concerning POM-based nanocomposites [19]. Hence, the aim of this work was to obtain and characterise novel POM-MMT nanocomposites.

EXPERIMENTAL

Materials

Polyoxymethylene (trade-name Tarnoform T-300, melt flow index 9 g/10 min) was produced by Zakłady Azotowe w Tarnowie-Mościcach SA, Poland.

MMT was kindly supplied by Zakłady Górniczo-Metalowe in Zębice, Poland.

Table 1. Characteristics of quaternary ammonium surfactants used in organomontmorillonite preparation

Chemical constitution of surfactant	Sample code
$\begin{array}{c} \text{CH}_3 \\ \\ \text{R}-\text{N}^{\oplus}-\text{CH}_3 \\ \\ \text{CH}_3 \end{array} \quad \text{Cl}^{\ominus}$	1R3M
$\begin{array}{c} \text{CH}_3 \\ \\ \text{R}_1-\text{N}^{\oplus}-\text{R}_2 \\ \\ \text{CH}_3 \end{array} \quad \text{Cl}^{\ominus}$	2R2M
$\begin{array}{c} \text{H}_2\text{C}-\text{CH}_2\text{OH} \\ \\ \text{R}-\text{N}^{\oplus}-\text{CH}_3 \\ \\ \text{H}_2\text{C}-\text{CH}_2\text{OH} \end{array} \quad \text{Cl}^{\ominus}$	RM2Et
$\begin{array}{c} \text{CH}_2-\text{CH}_2-\text{OH} \\ \\ \text{HO}-\text{C}_6\text{H}_4-\text{CH}_2-\text{N}^{\oplus}-\text{R} \\ \\ \text{CH}_2-\text{CH}_2-\text{OH} \end{array} \quad \text{Cl}^{\ominus}$	RB2Et
$\begin{array}{c} \text{CH}_3 \\ \\ \text{R}-\text{N}^{\oplus}-\text{CH}_3 \\ \\ \text{CH}_3 \end{array} \quad \text{Cl}^{\ominus}$	RA3M, where R contains amide group

The cationic surfactants were kindly provided by ICSO in Kędzierzyn-Koźle, Poland. The chemical structures of organic modifiers used in this work are presented in Table 1. The hydrocarbon constituents (R, R₁, R₂) contain 16–18 carbon atoms.

Modification of MMT

MMT (bentonite) was dispersed in hot distilled water. Water solution of a cationic surfactant was then

slowly added in a quantity adequate to cation exchange capacity of bentonite. The mixture was stirred for 3 hours to enable complete exchange of sodium cations into organic ones. Then the precipitate was filtered and washed with hot distilled water until no chloride ions were detected in the filtrate after addition of 0.1 mol AgNO_3 . Finally, the filtered cake was dried in the open air, grounded into fine powder and size-graded with 50 μm sieve. Before blending organomodified bentonites were dried overnight under vacuum at 90 $^\circ\text{C}$.

Preparation of POM-MMT nanocomposites

Nanocomposites were obtained by melt mixing of melted POM and inorganic filler using a Haake internal mixer allowing constant control of torque for 15 minutes at temperature of 180 $^\circ\text{C}$ at rotor speed 60 rpm. Laboratory pneumatic injection moulding machine was used in the second stage for preparation of injection moulded samples (the barrel temperature was 180 $^\circ\text{C}$ and the mould temperature was 70 $^\circ\text{C}$).

Characterization methods

— X-ray diffraction measurements were carried out on a Philips X-Pert diffractometer, with graphite monochromator placed in the front of detector ($\lambda_{\text{Cu}} = 1.5418 \text{ \AA}$).

— A scanning electron microscope SEM Philips XL30, equipped with detector of secondary electrons (SE), was used to investigate the surface morphology of carbon-coated samples at the energy of the electron beam of 10–15 kV.

— For DSC measurements a Netzsch DSC 200, operating in dynamic mode (heating = 10 K/min), was employed. Microslides of polymeric material with thickness of *ca.* 6 μm were cut by a microtome Leica RM2145 from surface and core regions of injection moulded samples. Samples of ~2.5 mg weight were placed in sealed aluminium pans. Prior to use the calorimeter was calibrated with indium and mercury standards.

— Thermogravimetric analysis was performed on a Netzsch TG 209 thermal analyser, operating in a dynamic mode at a heating rate of 10 K/min. The conditions were: sample weight — ~5 mg, atmosphere — argon, open $\alpha\text{-Al}_2\text{O}_3$ pan.

— Tensile properties were measured by a Zwick 1445 universal testing machine at the crosshead speed of 20 mm/min. The dimensions of the tested part of specimen were: thickness 1.5 mm, width 4.8 mm, length 25 mm (according to PN-EN ISO 527-2:1996 standard).

— Three point bending method was applied to determine the modulus of elasticity. In this method edge-supported material sample is loaded in the middle point perpendicularly to its centre line. The test conditions were in accordance with PN-79/C-89027 standard.

RESULTS AND DISCUSSION

Characterization of organo-modified montmorillonite

The process of organophilisation of montmorillonite was based on a cation exchange reaction of inorganic sodium ions into organic ammonium ions. This modification facilitates the dispersion of individual MMT layers by (i) changing the hydrophilic character of montmorillonite into organophilic one thus allowing macromolecules to intercalate into MMT galleries, and (ii) increasing the distances between montmorillonite layers and simultaneously weakening electrostatic forces responsible for MMT stack cohesion. In our study different surfactants were chosen to check both the effect of number of hydrocarbon chains (1R3M and 2R2M — see table 1) and the presence of various polar groups that were supposed to improve interactions between organic and inorganic materials (RM2Et, RB2Et and RA3M).

The maximum of diffraction peak observed by WAXD method for modified MMT was shifted towards lower values of 2θ angle in comparison to pristine montmorillonite (Fig. 2, curve b) — this observation confirms

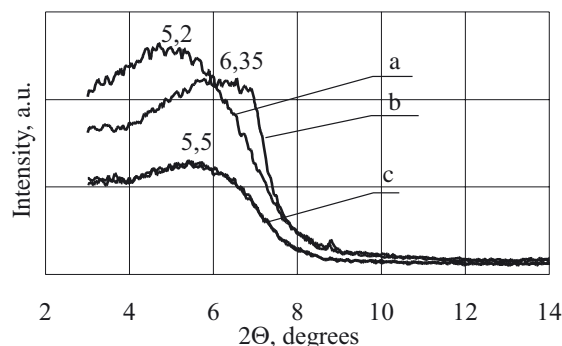


Fig. 2. XRD diffractograms of samples: a — MMT-RA3M, b — Na^+MMT , c — POM/MMT-2R2M

that an increase of gallery space due to the presence of surfactant molecules between MMT layers occurs. The position of peak scattered around 5.2° without showing a clear dependence on chemical structure of surfactant (e.g. Fig. 2, curve a).

Evaluation of nanocomposites

Structure

Nanostructure of POM-MMT nanocomposites was evaluated by WAXD method and there was a 2θ peak at *ca.* 5.5° (Fig. 2, curve c) indicating the presence of nonintercalated stacks of organomodified MMT layers. However, taking into account the weak intensity of these peaks, partial exfoliation of montmorillonite can be considered. Similar results of structure analysis were re-

ported for polyetherimide nanocomposites where material was initially described as immiscible but it had a large number of exfoliated single layers present [20]. Therefore, mixed structure is proposed for obtained POM/MMT nanocomposites containing both exfoliated regions and unintercalated microscale stacks of MMT.

One can consider peeling of external layers from the grain of montmorillonite filler as a mechanism ruling the MMT exfoliation in polymer matrix during melt mixing whereby the grain size could play a crucial role in MMT dispersing. It is notable that processing parameters such as time of mixing and share rates are restricted by limited thermal stability of polyoxymethylene, so grain size should be reduced as much as possible to obtain genuine nanocomposite structure.

Morphology

Considerable changes in morphology of injection moulded samples of nanocomposites as compared to pure POM were observed by SEM. Microphotographs of criofractured nanocomposite samples as well as rupture surface of samples after tensile tests revealed a core-shell morphology, where the core was built from bigger and regularly developed spherulites while shell exhibiting significantly increased thickness (in comparison to POM) was composed of small crystalline structures oriented towards the melt flow direction (Figs. 3 and 4).

To explain the possible mechanism of enhanced shell layer formation one should first discuss the spatial orientation of montmorillonite layers under melt flow conditions. Studies on the clay orientation using X-ray diffraction methods revealed that in external areas of injection moulded parts MMT layers are located parallel to the surface and to each other (regular structure) and inside the moulded sample nanolayers are arranged randomly [21]. Oriented polymer crystalline structures

were produced in POM/MMT nanocomposites in the shell area due to montmorillonite layers arrangement and under crystallization conditions involving supercooling and high pressures during melt flow. Similar strong sensitivity toward developing of core-shell morphology was discovered by Pecorini *et al.* in rubber-toughened polyoxymethylene [22].

DSC analysis

Table 2. Enthalpy of melting and crystallinity degree of POM and its compositions in core and shell region of injection moulded samples

Sample	Enthalpy of melting ΔH_m , J/g		Crystallinity degree X_c , %	
	core region	shell region	core region	shell region
POM	135.1	133.7	41.4	41.0
POM/Na ⁺ MMT (microcomposite)	145.4	136.8	44.6	41.9
POM/MMT-2R2M (nanocomposite)	168.0	137.6	51.5	42.2

Changes of POM crystallinity upon MMT addition were investigated by DSC method. In Table 2 values of melting enthalpy and crystallinity degree for core and shell regions of pure POM, composite of POM with unmodified sodium montmorillonite and POM/MMT-2R2M nanocomposite are collected. The degree of polymer matrix crystallinity was calculated according to the relationship:

$$X_c = \frac{\Delta H_m}{\Delta H_m^0} \cdot 100 \% \quad (1)$$

whereby: ΔH_m — enthalpy of melting [J/g], ΔH_m^0 — enthalpy of melting of 100 % crystalline POM (326 J/g) [23].

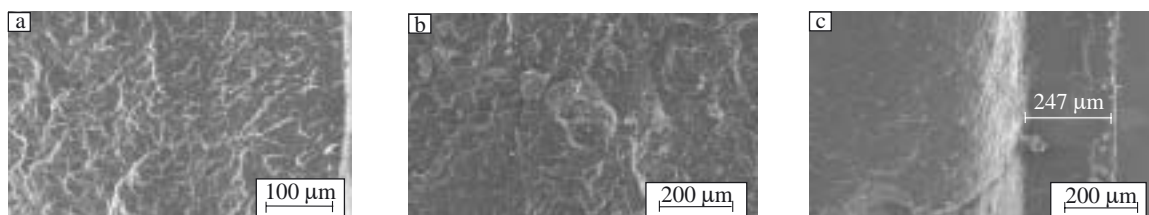


Fig. 3. SEM microphotographs of criofractured samples of a — POM, b — POM/Na⁺MMT and c — POM/MMT-2R2M

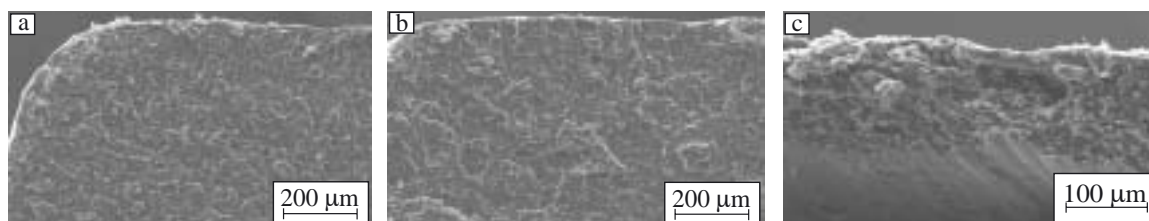


Fig. 4. SEM microphotographs of tensile fractured surface of a — POM, b — POM/Na⁺MMT and c — POM/MMT-2R2M

When MMT nanoparticles are dispersed in POM, significant increase in crystallinity degree occurs in the core area that can reflect the nucleation activity of montmorillonite. Effective nucleation of POM by silicate compound (attapulgite and diatomite) was previously reported by Xu and He work where fine-grain spherulites were formed [24]. The existence of many grooves and microvoids on the silicate surface that may absorb the chain or segment of POM due to well compatible chemical bonds of filler (Si-O) and polymer (C-O) were claimed to favor nucleation process. It is of interest to note that small changes in crystallinity degree are observed in shell parts of injection mould. One may consider effect of polymer chains capped between layers and supercooling conditions as factors counteracting the growth of crystalline phase [25].

Mechanical testing

The results of mechanical strength of POM/MMT nanocomposites, investigated by tensile and three point bending tests; are presented in Figs. 5–7. Tensile strength of POM/MMT nanocomposites showed an increasing tendency. The changes in modulus of elasticity indicated that the material became stiffer under MMT incorporation. The most important observation was that both tensile strength and ductility were improved after incorporation of MMT-2R2M. This is an important effect, contrary to classical microcomposites' behavior where increased mechanical strength at the expense of ductile properties usually occurs (see sample POM/MMT-Na⁺MMT).

Two major factors associated with the chemical structure of organomodifier could be taken into account when explaining mechanical performance of POM/MMT-2R2M nanocomposite material: the presence of two alkyl chains (i) facilitates proper dispersion of layered silicate because adherent coverage of surface layer effectively diminishes the cohesion forces of MMT stacks, and (ii) causes plasticization effect of macrochains improving thus material ductility.

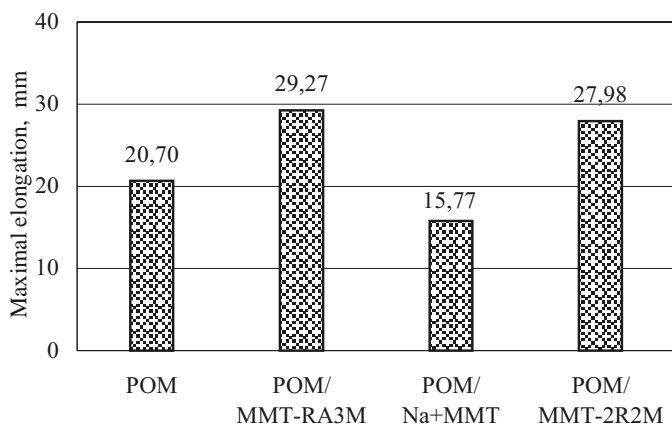


Fig. 5. Maximum elongation at break of POM and POM/MMT nanocomposites

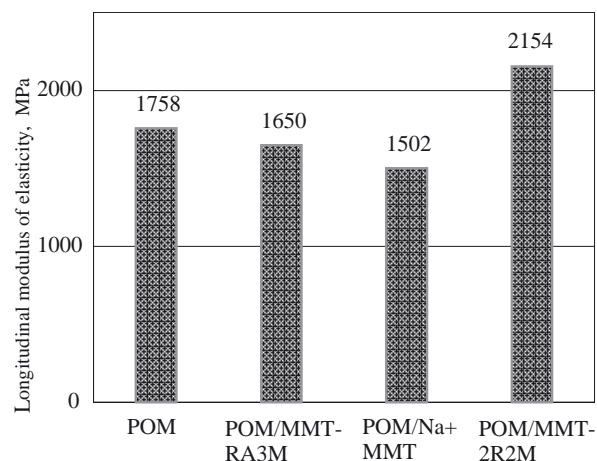


Fig. 6. Longitudinal (Young) modulus of elasticity of POM and POM/MMT nanocomposites

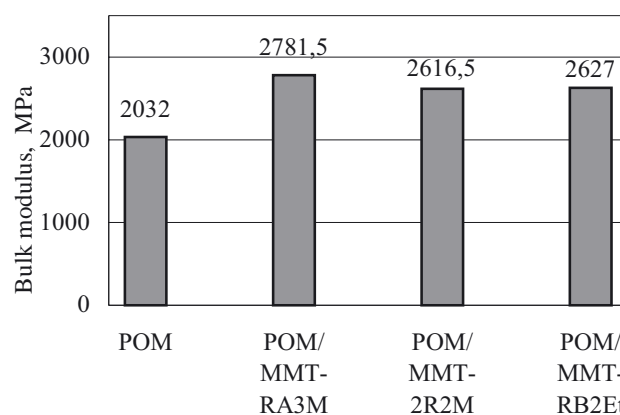


Fig. 7. Bulk modulus of elasticity of POM and POM/MMT nanocomposites

However, most probably the enhancement in mechanical performance of POM/MMT system was due to complex core-shell morphology of nanocomposite injection moulded tensile samples. Delaminated crystalline structures in a shape of plates located in shell layer of injection moulded samples after tensile tests indicated shear yielding mechanism of fracture while crazing should be expected to occur in core areas. The increase in shell thickness could be conducive to ductile behavior of POM/MMT nanocomposites. Pecorini's interpretation may be cited in support of this assumption [22].

Elsewhere, the influence of microstructure on mechanical properties of compression moulded and injection moulded samples of POM were compared by Plummer *et al.* [26]. They found injection moulded samples with finer microstructures that arisen from faster cooling rates exhibiting higher values of the plane-strain critical stress intensity K_{IC} for crack initiation. However, there was no evidence that crack paths followed the spherulite boundaries. The changes in K_{IC} value were linked to variations in the molecular density rather than to changes in microstructure.

Thermal stability

Thermogravimetric analysis was applied to ascertain the thermal stability of POM materials and it has been found that the thermal decomposition of alkyl ammonium compounds starts around 200 °C that is close or even below processing temperature of polyoxymethylene (Fig. 8, Table 3). It has been shown by Delozier *et al.* that when organic compound used for MMT modifica-

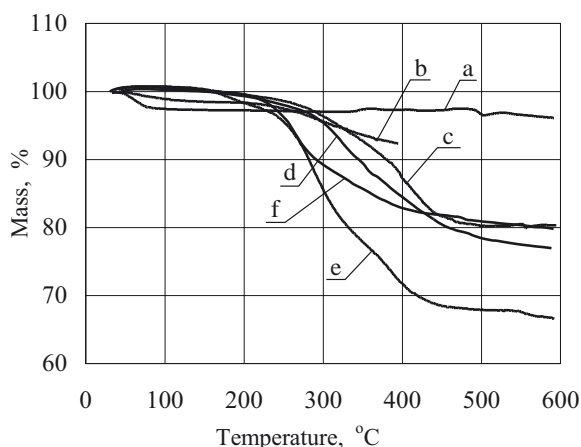


Fig. 8. TG profiles of pure sodium montmorillonite and organo-modified montmorillonites: a — Na⁺MMT, b — MMT-1R3M, c — MMT-RM2Et, d — MMT-RA3M, e — MMT-2R2M, f — MMT-RB2Et

tion undergoes thermal degradation during processing, the galleries of layered silicate will collapse and the filler will become hydrophilic [27]. This process counteracts the intercalation and immiscible composites are more likely to be formed. Furthermore, during thermal degradation of alkylammonium compounds intercalated into MMT galleries that proceeds according to the Hoffman mechanism, the ammonium cation loses an olefin and an amine, and leaves an acid proton on the surface of the MMT [28].

Table 3. TG results of POM-based nanocomposites

Sample	T ₁₀ %, °C	T _{max} , °C	Char at 600 °C, %
POM	313	333	0.9
POM/Na ⁺ MMT	245	274	3.8
POM/MMT-2R2M	274	295	8.5
POM/MMT-RA3M	254	278	4.0
POM/MMT-3M1R	256	285	4.3
POM/MMT-RB2Et	239	259	1.9

The thermal stability of the obtained nanocomposites was strongly influenced by the presence of organo-modified MMT — the initial decomposition temperatures were significantly lowered, an effect that can be ascribed to acceleration of POM decomposition process by gase-

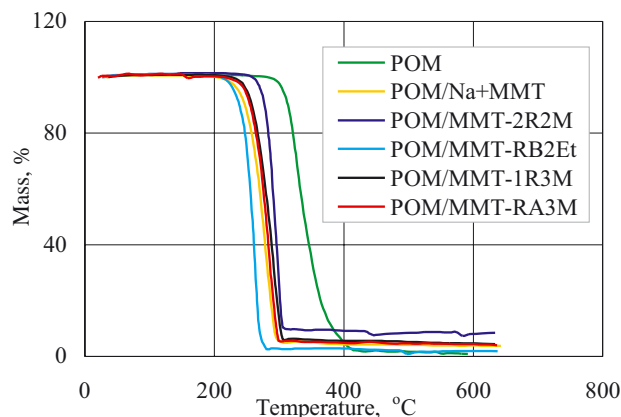


Fig. 9. TG profiles of polyoxymethylene and its composites

ous products of ammonium compound degradation, as well as by acidic protons left on MMT surface after alkyl ammonium volatilisation (Fig. 9). The presence of ammonium compounds causes also a more rapid decomposition at the next stages of process. A crucial observation of enhanced char formation was done during POM/MMT-2M2R nanocomposite degradation — 8.5 wt. % of residue was left at 600 °C. POM/MMT-2M2R nanocomposite contains organo-modified MMT that incorporates the highest amount of organic modifier and provides an excellent dispersion of MMT layers in polymer matrix. Enhanced char formation is of paramount importance for flame retardation and the observed effect will be further investigated.

CONCLUSIONS

The introduction of MMT into POM matrix enhanced significantly different properties and the performance of the obtained materials varied with composition as well as with degree of exfoliation of MMT layers. Changes in morphology of injection moulded nanocomposite samples were ascribed to different orientation of MMT layers, influencing thus mechanical properties. Thermal stability of organic modifier was considered as an important parameter governing the dispersibility of o-MMT, but it was also a limiting factor for processing. An important effect of enhanced char formation is to be exploited for further flame retardation.

ACKNOWLEDGMENT

Authors are grateful to the Polish State Committee for Scientific Research for financial support under grant PBZ-KBN-095/T08/2003.

REFERENCES

1. Forschirm A., McAndrew F. C.: "Polymeric Materials Encyclopedia", CRC Press, New York 1996.
2. Pielichowski K., Leszczynska A.: *J. Polym. Eng.* 2005, 4, 359.

3. Mamunya Y. P., Muzychenko Y. V., Possis P., Lebedev E. V., Shut M. I.: *J. Macromol. Sci.-Phys.* 2001, **B40**, 591.
4. Sinha Ray S., Okamoto M.: *Prog. Polym. Sci.* 2003, **28**, 1539.
5. Oleksy M., Heneczkowski M.: *Polimery* 2005, **50**, 143.
6. Pinavaia T. J., Beall G. W.: "Polymer-Clay Nanocomposites", John Wiley & Sons, Chichester 2000.
7. Njuguna J., Pielichowski K.: *Adv. Eng. Mat.* 2004, **6**, 204.
8. Kelar K., Jurkowski B., Mencil K.: *Polimery* 2005, **50**, 449.
9. Yoon P. J., Hunter D. L., Paul D. R.: *Polymer* 2003, **44**, 5323.
10. Ke Y., Long C., Qi Z.: *J. Appl. Polym. Sci.* 1999, **71**, 1139.
11. Gilman J.: *J. Appl. Clay Sci.* 1999, **15**, 31.
12. Vaia R. A., Price G., Ruth P. N., Nguyen H. T.: *J. Appl. Clay Sci.* 1999, **15**, 67.
13. Nour M. A., Hassanien M. M.: *Polimery* 2005, **50**, 371.
14. Messersmith P., Giannelis E.: *J. Polym. Sci., Polym. Chem.* 1995, **33**, 1047.
15. Usuki A., Kojima Y., Kawasumi M., Okada A., Fukushima Y., Kurauchi T., Kamigaito O.: *J. Mater. Res.* 1993, **8**, 1179.
16. Hasegawa N., Okamoto H., Kato M., Usuki A., Sato N.: *Polymer* 2003, **44**, 2933.
17. Pawlak A., Morawiec J., Piórkowska E., Gałęski A.: *Polimery* 2004, **49**, 240.
18. Sinha Ray S., Okamoto K., Okamoto M.: *Macromolecules* 2003, **36**, 2355.
19. Xu W., Ge M., He P.: *J. Appl. Polym. Sci.* 2001, **82**, 2281.
20. Morgan A. B., Gilman J. F.: *J. Appl. Polym. Sci.* 2003, **87**, 1329.
21. Yu Z.-Z., Yang M., Zhang Q., Zhao C., Mai Y.-W.: *J. Appl. Polym. Sci.: Part B: Polym. Phys.* 2003, **41**, 1234.
22. Pecorini T. J., Hertzberg R. W., Manson J. A.: *J. Mater. Sci.* 1990, **25**, 3385.
23. Sauer B. B., McLean R. S., Londono J. D.: *J. Macromol. Sci. — Phys.* 2000, **B40**, 519.
24. Xu W., He P.: *J. Appl. Polym. Sci.* 2001, **80**, 304.
25. Kim G.-M., Lee D.-H., Hoffmann B., Kressler J., Stöppelmann G.: *Polymer* 2001, **42**, 1095.
26. Plummer C. J. G., Menu P., Curdé-Maurox N., Kausch H.-H.: *J. Appl. Polym. Sci.* 1995, **55**, 489.
27. Delozier D. M., Orwoll R. A., Cahoon J. F., Johnston N. J., Smith Jr. J. G., Connell J. W.: *Polymer* 2002, **43**, 813.
28. Xie W., Gao Z. M., Pan W. P., Hunter D., Singh A., Vaia R. A.: *Chem. Mater.* 2001, **13**, 2979.